ACS Catalysis

Research Article

pubs.acs.org/acscatalysis

Isostructural Zeolite-Supported Rhodium and Iridium Complexes: Tuning Catalytic Activity and Selectivity by Ligand Modification

Claudia Martinez-Macias, Pedro Serna, and Bruce C. Gates*

Department of Chemical Engineering and Materials Science, University of California, Davis, California 95616, United States

Supporting Information

ABSTRACT: A family of isostructural, essentially molecular complexes of rhodium and of iridium anchored to HY zeolite was synthesized from $M(C_2H_4)_2(acac)$ and $M(CO)_2(acac)$ (M = Rh, Ir; acac is acetylacetonate), with the initial supported species being $M(C_2H_4)_2$ and $M(CO)_2$, each bonded to the zeolite through two M−O bonds. Each was used as a catalyst at 300 and 373 K and atmospheric pressure for the conversion of ethylene in the presence of H_2 (and sometimes D_2), giving ethane and, when the metal was rhodium, butenes, and, when D_2 was present, HD. The high degree of uniformity of the metal complexes allowed a precise spectroscopic elucidation of the predominant species present during catalysis. The CO ligands were inhibitors of the catalytic reactions, with the metal dicarbonyl complexes lacking measurable activity under our conditions. The CO ligands also served as probes helping to characterize the structures and electronic properties of the catalytic metal complexes. The data show that subtle changes in the bonding of the ligands markedly affect the catalytic performance.

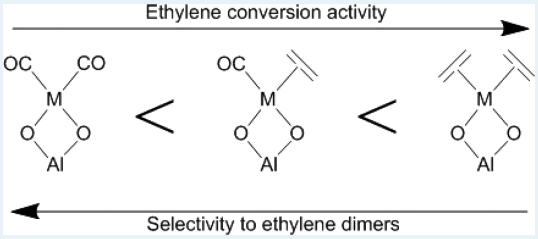

KEYWORDS: *iridium carbonyl complexes, rhodium carbonyl complexes, zeolite-supported metal, ethylene hydrogenation, ethylene dimerization*

INTRODUCTION

New and improved molecular organometallic catalysts often emerge from tests involving variation of ligands to optimize their steric and electronic effects. When a metal is anchored to a support such as a metal oxide, the same principles and methods apply, but it is challenging to vary the ligands without changing other properties, such as the metal nuclearity.[1,2] The opportunities are limited by the number of coordination sites on the metal—with the support itself being a ligand that often occupies more than one coordination site[3] and influences the catalytic activity.[4,5] Reports of families of supported mononuclear metal complexes with well-defined structures, including isostructural complexes of rhodium and of iridium with various ligands, have become available,[6−8] and these now allow experiments with systematically varied ligands to determine how the ligands influence the catalytic properties.

Here, we report structure-catalytic property relationships determined for isostructural supported rhodium and supported iridium complexes used to catalyze reactions of ethylene and H_2. The support was chosen to be a zeolite, because its crystalline structure allows the formation of structurally uniform supported species. The ligands, in addition to the zeolite support and those derived from the reactants ethylene and H_2, include CO, which is so strongly bonded that it poisons metal catalysts in many forms; it is also a coreactant in some reactions (e.g., alkene hydroformylation[9]) and a π-acid ligand that regulates reactivity through electronic effects. In some instances, CO also stabilizes supported metals in the form of mononuclear species by limiting their reduction and aggregation into clusters (which are oxidatively fragmented by CO).[10−12] CO is used to tune the properties of supported catalysts in industrial reactions such as alkene polymerization,[13] and it is a selective poison that markedly improves the selectivities of some catalysts.[14] Ethylene conversion in the presence of H_2 was chosen to probe the catalyst performance, because (1) it takes place under mild conditions without reduction and aggregation of the metals;[3] (2) it allows measurement of both activity and selectivity data, as both hydrogenation and dimerization of the ethylene take place (at least with some catalysts); (3) the reactants are small and provide spectroscopic signatures that help in the identification of the ligands bonded to the metals.[13,15]

We emphasize a contrast between the inherent complexity of the surfaces of conventional solid catalysts (which makes it difficult to resolve the effects of ligands on catalytic performance[16]) and essentially molecular supported metal complexes such as ours—species that are synthesized precisely on nearly uniform crystalline supports and thereby provide excellent opportunities for resolution of ligand effects.[3]

The data reported here allow an evaluation of ligand effects with zeolite-supported rhodium carbonyl complexes and iridium carbonyl complexes for the conversion of H_2 with D_2 to give HD and for the conversion of ethylene + H_2 to give ethane and, in some cases, also butenes as catalytic reaction products. The activity and selectivity of our catalysts were measured to elucidate the ligand effects under conditions mild

Received: May 13, 2015
Revised: August 13, 2015
Published: August 18, 2015

DOI: 10.1021/acscatal.5b00995
ACS Catal. 2015, 5, 5647−5656

Table 1. Summary of EXAFS Fit Parameters[a] and Vibrational Frequencies Characterizing HY-Zeolite-Supported Complexes of Rhodium and of Iridium

		EXAFS parameters						
sample precursor	sample/treatment conditions	absorber-backscatterer pair	N	R (Å)	$10^3 \times \Delta\sigma^2$ (Å^2)	ΔE_0 (eV)	IR bands in the ν_{CO} region of supported species (cm^{-1})	supported metal species inferred from data
$Ir(C_2H_4)_2(acac)$	$Ir(C_2H_4)_2$ in helium at 298 K	$Ir-O_{zeolite}$	2.1	2.11	3.8	−4.7	[b]	$Ir(C_2H_4)_2$
		$Ir-C_{C2H4}$	4.0	2.03	8.9	−5.9		
		$Ir-Al_{zeolite}$	1.0	3.01	4.3	−6.7		
$Ir(CO)_2(acac)$	$Ir(CO)_2$ in helium at 298 K	$Ir-O_{zeolite}$	2.0	2.06	2.7	−3.4	2109, 2038	$Ir(CO)_2$
		$Ir-C_{CO}$	2.0	1.97	6.3	3.6		
		$Ir-O_{CO}$	2.0	2.94	8.3	−7.7		
		$Ir-Al_{zeolite}$	0.9	2.73	3.1	2.4		
$Ir(CO)_2(acac)$	sample formed from $Ir(CO)_2$ after treatment in C_2H_4 at 298 K	$Ir-O_{zeolite}$ and $Ir-C_{C2H4}$	4.5	2.01	7.5	−2.2	2087	$Ir(CO)(C_2H_4)_2$
		$Ir-C_{CO}$	1.0	1.83	3.0	0.1		
		$Ir-O_{CO}$	1.0	2.95	3.4	−6.4	2055	$Ir(CO)(C_2H_4)$
		$Ir-Al_{zeolite}$	1.0	2.77	3.7	1.0		
$Ir(CO)_2(acac)$	sample formed from $Ir(CO)_2$ after treatment in C_2H_4 at 373 K	$Ir-O_{zeolite}$	4.0	2.01	9.5	−0.7	2055	$Ir(CO)(C_2H_4)$
		$Ir-C_{CO}$	1.0	1.85	4.2	5.5		
		$Ir-O_{CO}$	1.0	3.01	5.8	−7.6		
		$Ir-Al_{zeolite}$	1.0	2.87	6.45	−3.0		
$Rh(C_2H_4)_2(acac)$	$Rh(C_2H_4)_2$ in helium at 303 K[c]	$Rh-O_{zeolite}$	2.1	2.15	3.1	7.1	[b]	$Rh(C_2H_4)_2$
		$Rh-C_{C2H4}$	3.7	2.08	3.4	−2.0		
		$Rh-Al_{zeolite}$	1.1	3.02	6.7	−2.5		
$Rh(CO)_2(acac)$	$Rh(CO)_2$ in helium at 298 K	$Rh-O_{zeolite}$	1.9	2.17	4.8	−7.9	2117, 2053	$Rh(CO)_2$
		$Rh-C_{CO}$	1.9	1.82	4.4	4.1		
		$Rh-O_{CO}$	1.9	3.01	1.7	−7.0		
		$Rh-Al_{zeolite}$	1.0	3.17	0.0	2.0		
$Rh(CO)_2(acac)$	sample formed from $Rh(CO)_2$ after treatment in C_2H_4 at 298 K	$Rh-O_{zeolite}$ and $Rh-C_{C2H4}$	4.0	2.22	5.9	2.8	2056	$Rh(CO)(C_2H_4)$
		$Rh-C_{CO}$	1.0	1.79	2.9	3.4		
		$Rh-O_{CO}$	1.0	3.00	0.6	−2.5	2062 (shoulder)	rhodium carbonyl complex
		$Rh-Al_{zeolite}$	1.0	3.14	1.9	7.2		

[a]Notation: N, coordination number; R, distance between absorber and backscatterer atoms; $\Delta\sigma^2$, disorder term (Debye−Waller factor); ΔE_0, inner potential correction. Error bounds characterizing the structure parameters obtained by EXAFS spectroscopy are estimated to be as follows: $N \pm 20\%$; $R \pm 0.02$ Å; $\Delta\sigma^2 \pm 20\%$; inner potential correction $\Delta E_0 \pm 20\%$. The errors in the Ir−Al contributions are larger than those characterizing the other contributions, and the data are not sufficient for good estimates of the uncertainties in the former values. The accuracy of the Debye−Waller factor for the $M-C_{CO}$ and $M-O_{CO}$ contributions ($\pm 1 \times 10^{-3}$ Å^2) implies that the mean M−C−O angle of the rhodium and iridium complexes is approximately equal to the angle in the reference complexes.[21] [b]No IR bands were evident in this region. [c]Data reported previously.[22]

enough to prevent formation of clusters of the supported metals. Catalyst structures were characterized by infrared (IR), X-ray absorption near edge (XANES), and extended X-ray absorption fine structure (EXAFS) spectroscopies, and some of the spectra were recorded to help identify the ligands present on the metals in working catalysts.

EXPERIMENTAL METHODS

Materials, Sample Preparation, and Handling. Dealuminated zeolite HY (Zeolyst International, CBV760, Si/Al atomic ratio ≅ 30 according to the manufacturer) was calcined in O_2 (Praxair, 99.5%) at 773 K for 2 h, followed by evacuation at 773 K for 14 h. After calcination, the support was stored in an argon-filled glovebox (MBraun, with H_2O concentrations <0.5 ppm and O_2 concentrations <1 ppm). Standard Schlenk line and inert-atmosphere glovebox methods for handling air- and moisture-sensitive materials were used for catalyst syntheses with the following precursors: $Rh(CO)_2(acac)$ (acac is acetylacetonate; 99%, Strem), $Rh(C_2H_4)_2(acac)$ (99%, Strem), $Ir(CO)_2(acac)$ (99%, Strem), and $Ir(C_2H_4)_2(acac)$ (synthesized as described elsewhere[17]), all of them fully characterized previously either by the manufacturer or in published results.[17] Each separate precursor and the calcined zeolite were combined into a slurry with dried and deoxygenated *n*-pentane (Fisher, 99%) and stirred for 24 h. The solvent was then removed by evacuation for a day; the compositions of the synthesis mixtures were chosen to give 1 wt % rhodium or iridium in the resultant powder samples. Samples were stored in the glovebox. The resultant samples' colors were the following: $Rh(C_2H_4)_2$/zeolite, light yellow; $Ir(C_2H_4)_2$/zeolite, pale yellow; and $Rh(CO)_2$/zeolite and $Ir(CO)_2$/zeolite, light gray. H_2 was supplied by Airgas (99.999%) and purified by passage through traps containing reduced Cu/Al_2O_3 and activated zeolite 4A to remove traces of O_2 and moisture, respectively. Helium (Airgas, 99.999%) and ethylene (Airgas, 99.5%) were purified by passage through similar traps. CO in a 10 mol % mixture in helium was purified by passage through a trap containing particles of activated γ-Al_2O_3 and of zeolite 4A to remove any traces of metal carbonyls from high-pressure gas cylinders and moisture, respectively. D_2 (99.8%) was purchased from Cambridge Isotope Laboratories.

Infrared Spectroscopy. IR spectra of catalysts were recorded with a Bruker IFS 66v/S spectrometer; the spectral resolution was 2 cm^{-1}. Each sample (~30 mg) was pressed into a thin wafer and loaded between two KBr windows in a cell in the argon-filled glovebox. The cell was sealed, transferred, and connected to a flow system that allowed recording of spectra while gases flowed through and around the sample. Air and

DOI: 10.1021/acscatal.5b00995
ACS Catal. 2015, 5, 5647−5656

moisture were excluded. Spectra were recorded at various temperatures in the presence of various flowing gases. Each reported spectrum is the average of 64 scans.

Mass Spectrometry. Mass spectra of the effluent gases from the flow system, including components formed by reaction with the catalyst sample, were measured with an online Balzers OmniStar mass spectrometer running in multi-ion monitoring mode. The data were collected as IR spectra were being recorded. Changes in the signal intensities of H_2 (m/z = 2), HD (m/z = 3), D_2 (m/z = 4), CO (m/z = 28), C_2H_4 (m/z = 28, 27, 26), C_2H_6 (m/z = 30, 28, 27, 26), and C_4H_8 (m/z = 55, 41) were recorded.

Catalytic Reaction of H_2 with D_2 in a Flow-through Infrared Cell. The catalytic reaction of H_2 with D_2 to give HD was carried out with each catalyst (~30 mg) in the IR cell, which served as a once-through flow reactor; the catalyst was loaded into the reactor in the glovebox. The feed components were ethylene, H_2, and/or D_2, with ratios of 1:1 H_2/D_2 and 2:1 H_2/C_2H_4. The reaction was performed at atmospheric pressure and a temperature of 298 or 373 K, and the products were analyzed by mass spectrometry.

Catalytic Reaction of Ethylene with H_2 in a Once-Through Tubular Flow Reactor. A selected mass of catalyst (4−240 mg) was mixed with particles of inert, nonporous α-Al_2O_3 (10 g), and the mixture was placed in a conventional once-through thermostated tubular plug-flow reactor. The reaction mixture (H_2 + C_2H_4, molar ratio = 4.0) flowed through the catalyst bed at atmospheric pressure and a temperature of 300 or 373 K. The effluent stream was analyzed periodically with an online gas chromatograph (Hewlett−Packard HP-6890) equipped with a capillary column (PLOT Alumina "M," 50 m × 0.53 mm) and a flame-ionization detector. Conversions of ethylene were typically in the differential range, shown experimentally to be <8%.

X-ray Absorption Spectroscopy. X-ray absorption spectra of catalyst samples were recorded at beamline 10-ID-B (MR-CAT) at the Advanced Photon Source (APS) at Argonne National Laboratory and at beamline 4-1 at the Stanford Synchrotron Radiation Lightsource (SSRL). At APS, the storage-ring electron energy and ring current were 7 GeV and 105 mA, respectively, and the monochromator was a double-crystal Si(111). At SSRL, the storage-ring electron energy and ring current were 3 GeV and 300 mA, respectively, and the monochromator was a double-crystal Si(220). At each beamline, the monochromator was detuned by 20% at the Rh K edge or at the Ir L_{III} edge to minimize the effects of higher harmonics in the X-ray beam. Each powder sample inside an argon-filled glovebox at the synchrotron was loaded and sealed into a cell that served as a flow reactor.[18] Spectra were collected in transmission mode in the presence of flowing gases at atmospheric pressure and temperatures of 298 or 373 K. At SSRL, XANES and EXAFS spectra were recorded at intervals of 4 and 20 min, respectively, and at the APS, EXAFS spectra (including XANES spectra) were recorded at intervals of 4 min.

RESULTS

Synthesis and Characterization of Supported Catalyst Precursors. Samples prepared from the precursors M-$(C_2H_4)_2$(acac) (M = Rh, Ir) were synthesized as before.[6,7] IR (Figures S1−S3, Supporting Information) and EXAFS data (Table 1) show that the supported species were $M(C_2H_4)_2$, with each metal atom bonded, on average and within error, to two oxygen atoms of the zeolite support, as expected.[6,7]

IR and EXAFS spectra identify the supported catalyst precursors prepared from $Rh(CO)_2$(acac) and $Ir(CO)_2$(acac), respectively, as $Rh(CO)_2$/HY zeolite and $Ir(CO)_2$/HY zeolite. EXAFS data (Table 1) show that each metal was anchored to the support, on average and within error, through two M−O bonds (M = Rh, Ir) at tetrahedral zeolite Al sites, as shown at the left in Scheme 1. Thus, the metals in each catalyst were site

Scheme 1. Simplified Representation of the Zeolite-anchored Metal Dicarbonyl Complexes after Exposure to Ethylene at 298 K and 1 bar[a]

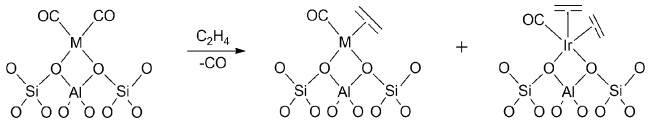

[a]The structure at the right was observed only for the iridium; there is no evidence of $Rh(CO)(C_2H_4)_2$, either from IR or EXAFS spectroscopy, under our conditions.

isolated. The spectra (Figures S4, S5) were used to determine structure data, which match those reported.[6,7] The sym/asym ratio for the zeolite-supported $M(CO)_2$ species suggests that the OC−M−CO angle is greater than 90° (99° for $Rh(CO)_2$ and 111° for $Ir(CO)_2$ species), consistent with previous reports,[19] and this angle differs from that corresponding to analogous species[20] bonded to less electron-withdrawing, nonporous supports. The acac dissociated from the precursors and adsorbed preferentially near Al^{3+} sites,[23,24] as was found in previous work with supported organometallic complexes such as ours.[25,26] Removal of the acac ligand from the metal precursor upon interaction with the zeolite surface is further demonstrated by the acac fingerprint region of the IR spectra, which shows bands at 1596, 1539, and 1366 cm^{-1}, which are characteristic of Hacac bonded to the zeolite (assigned to ν_{COring}, ν_{C-C-C}, and δ_{CH}, respectively, Figures S1B, S3C, S4C, and S5C in the Supporting Information). The spectra of both the rhodium and iridium dicarbonyl species include weak bands attributed to species other than the metal *gem*-dicarbonyls; the rhodium samples show satellite species indicative of CO with isotopes other than the common ones, and the iridium samples are characterized by a band assigned to iridium tricarbonyl species; during the following treatments, those bands disappeared.

Atomic-resolution images recorded with scanning transmission electron microscopy with samples synthesized as ours were from $Ir(C_2H_4)_2$(acac) and the zeolite showed that the iridium was atomically dispersed. All the spectroscopic evidence indicated that the cationic iridium complexes were bonded at the Al sites of the zeolite (the cation exchange sites).[29]

Treatment of each supported $M(CO)_2$ complex with flowing ethylene at 298 K and atmospheric pressure gave supported $M(CO)(C_2H_4)$ complexes (Scheme 1), characterized by IR and EXAFS spectra at the rhodium K and iridium L_{III} edges, respectively, as follows: the initial ν_{CO} bands assigned to the $M(CO)_2$ vibrations (2109 and 2038 cm^{-1} for iridium and 2117 and 2053 cm^{-1} for rhodium, Figures S6 and S7) disappeared within 4 min with the simultaneous growing in of new bands for iridium at 2087 and 2055 cm^{-1} (assigned to $Ir(CO)(C_2H_4)_2$ and $Ir(CO)(C_2H_4)$ complexes, respectively,[3] Figure S6) and for rhodium a band at 2056 cm^{-1} (assigned to $Rh(CO)(C_2H_4)$ complexes[6]) with a shoulder at approximately 2062 cm^{-1} (assigned to rhodium carbonyl species interacting with

DOI: 10.1021/acscatal.5b00995
ACS Catal. 2015, 5, 5647−5656

Table 2. Catalytic Reaction Data Characterizing HY Zeolite-supported Rhodium Complexes and Iridium Complexes for the Conversion of Ethylene at Atmospheric Pressure[a]

T (K)	metal complex initially present on HY zeolite support	feed composition (H_2/C_2H_4 molar ratio)	TOF in ethylene conversion[b] (s^{-1})	selectivity for dimers in ethylene conversion (mol %)	activity for H−D exchange (% conversion)	ref
300	$Rh(C_2H_4)$	4:1	0.26 ± 0.03	65 ± 7	3.5[c]	this work
303		4:1	0.26 ± 0.02	73 ± 4	*e*	22, 27
298		4:1	0.39 ± 0.12	76 ± 8	*e*	28
300	$Ir(C_2H_4)_2$	4:1	0.53 ± 0.09	11 ± 2	48[c]	this work
298		4:1	0.43 ± 0.17	28 ± 17	*d*	28
300		2:1	0.69 ± 0.08	*d*	11[e]	7
303		2:1	0.71 ± 0.09	*d*	11[e]	29
300	$Rh(CO)(C_2H_4)$	4:1	$4.1 \times 10^{-2} \pm 0.3 \times 10^{-2}$	10 ± 2	7.3[c]	this work
300	$Ir(CO)(C_2H_4)$	4:1	$5 \times 10^{-3} \pm 0.7 \times 10^{-3}$	*f*	3.4[c]	this work
		4:1	*d*	*d*	0.27[e]	7
373	$Rh(CO)(C_2H_4)$	4:1	*g*	*f*	66[c]	this work
373	$Ir(CO)(C_2H_4)$	4:1	1.52 ± 0.18[e]	*f*	36[c]	this work
		2:1		*d*	0.63[e]	7
300	$Rh(CO)_2$	4:1	*f*	*f*	*f*	this work
300	$Ir(CO)_2$	4:1	*f*	*f*	*f*	this work

[a]Reaction conditions: 1 bar; C_2H_4 and H_2 were present with helium at a partial pressure of 0.5 bar. [b]Turnover frequency (TOF) determined for catalyst in initial form. [c]Conversions reported after 8 min of contact with C_2H_4 + H_2 + D_2 at 1:2:2 molar ratios when the HD signal was constant. [d]Value not reported. [e]Data represented[16] as conversions relative to the equilibrium conversion. [f]Value too low to measure. [g]Value outside differential conversion range. To rule out the possibility of mixing effects in the catalytic reaction experiments, N_2 as a tracer was passed through the reactor to determine a characteristic purging time, which was about 3 min; all the catalytic measurements were taken at longer times on stream.

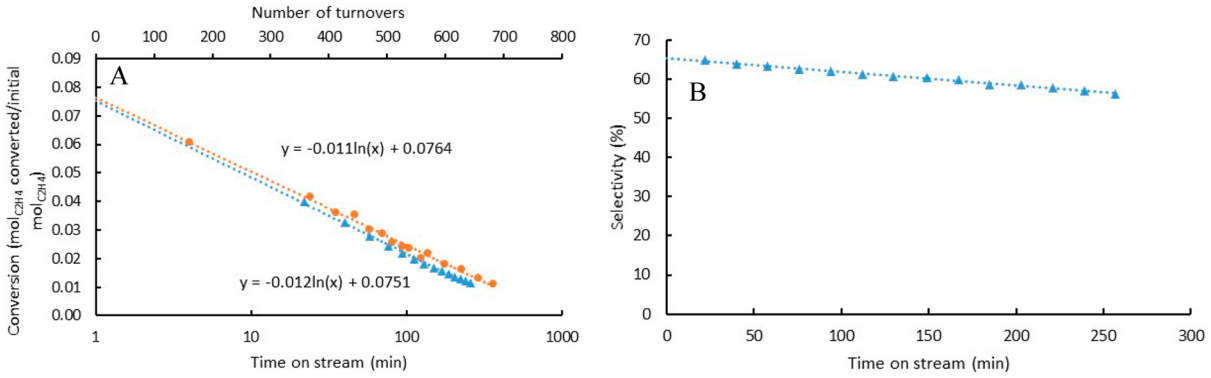

Figure 1. Performance of HY zeolite-supported $Rh(C_2H_4)_2$ complexes in the tubular flow reactor, with illustration of extrapolations to determine (A) initial conversions and (B) initial selectivity to ethylene dimers. Data were obtained at 300 K (▲) and 303 K (●)[22−27] and atmospheric pressure. The catalyst was in flowing helium before contact with C_2H_4 + H_2. The gas flow was 40 mL/min of H_2 and 10 mL/min of ethylene with balance helium of 50 mL/min. The catalyst mass was 21 mg, and the rhodium content 1 wt %.

ethylene,[6] Figure S7, Supporting Information). Complementing these results, EXAFS data (Table 1; also see the Supporting Information, Tables S2−S6 and Figures S23−S27) show that the $M-C_{CO}$ and $M-O_{CO}$ coordination numbers decreased from nearly 2 to nearly 1 as a result of the treatments in ethylene, indicating the removal of one of the two CO ligands initially present on each metal complex. At the same time, the coordination number of the EXAFS contribution characterizing the sum of the $M-O_{zeolite}$ + $M-C_{ethylene}$ (the data were not sufficient to resolve these two contributions) increased from nearly 2 to nearly 4.5 for the iridium complexes and from nearly 2 to nearly 4 for the rhodium complexes. These data indicate the replacement of the carbonyl ligand by ethylene, similar to reported data characterizing the exchange of one of the carbonyl ligands in metal *gem*-dicarbonyl species.[30,31]

In the case of the iridium, the fractional value suggests a mixture of species, consistent with the IR evidence of two species (Figure S6). The EXAFS spectroscopy-determined coordination number of nearly 4 for the combined $Rh-O_{zeolite}$ + $Rh-C_{ethylene}$ contribution, in contrast, suggests that the rhodium complex incorporated, on average, one ethylene ligand. The shoulder in the IR spectrum at approximately 2062 cm^{-1} (Figure S7) is assigned to rhodium carbonyl complexes (considered again below) present at too low a concentration to be distinguished from the $Rh(CO)(C_2H_4)$ species with EXAFS spectroscopy. Removal of the second CO ligand from the initially supported $M(CO)_2$ complexes in the presence of ethylene is much more difficult and was not observed under the mild experimental conditions investigated in this work. In contrast, when the initially supported $M(C_2H_4)_2$ complexes were brought in contact with CO, both ethylene ligands were quickly replaced by CO. All of these results are supported by IR and EXAFS data.[7]

The XANES data characterizing the supported $M(CO)_2$, $M(CO)(C_2H_4)$, and $M(C_2H_4)_2$ species (Figures S8,S9) give evidence of various ligands bonded to the metal, consistent

DOI: 10.1021/acscatal.5b00995
ACS Catal. 2015, 5, 5647−5656

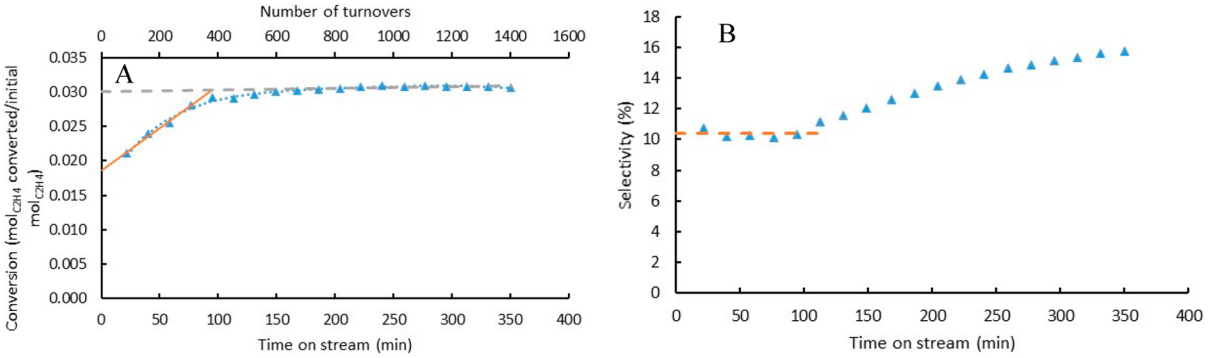

Figure 2. Performance of catalyst incorporating complexes initially in the form of $Rh(CO)(C_2H_4)_2$ supported on HY zeolite in a plug flow reactor, with illustration of methods of extrapolation to determine (A) initial conversion and (B) initial selectivity to ethylene dimers; data were obtained at 300 K and atmospheric pressure. To form the precatalyst, $Rh(CO)_2$ was exposed to a stream of ethylene (50 mL/min) for 60 min to form $Rh(CO)(C_2H_4)$, which was then brought in contact with $C_2H_4 + H_2$. When only ethylene flowed, no activity was observed. The feed gas flow rates were 40 mL/min of H_2, 10 mL/min of ethylene, and 50 mL/min of helium; the catalyst mass was 33 mg. The rhodium content 1 wt %.

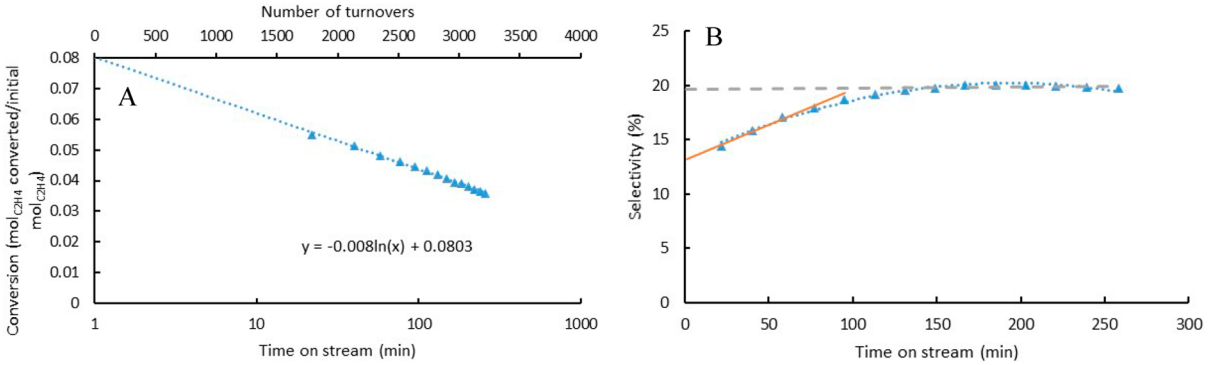

Figure 3. Performance of catalyst initially incorporating $Ir(C_2H_4)_2$ complexes supported on HY zeolite in a plug-flow reactor, with illustrations of the extrapolations to determine (A) initial conversion and (B) selectivity to ethylene dimers. The data were obtained at 300 K and atmospheric pressure. The gas feed flow rates were 40 mL/min of H_2, 10 mL/min of ethylene, and 50 mL/min of helium; the catalyst mass was 21 mg. The iridium content 1 wt %.

with the IR and EXAFS data. The lack of observable differences in the rhodium K-edge energies and iridium L_{III} edge energies, respectively characterizing the rhodium and iridium families of samples, indicate that the metal in each rhodium or iridium complex was in essentially the same oxidation state, independent of the ligands. These results are consistent with previous work and the inference of Rh(I) and Ir(I) complexes.[6,7]

Performance of Supported Rhodium Complex Catalysts. The rhodium complexes initially incorporating two CO ligands per Rh atom had immeasurably low catalytic activities for the conversion of ethylene + H_2 and for the H−D exchange under our conditions, as inferred from the GC and mass spectrometric data recorded at short times on stream (temperature, 300 or 373 K; pressure, atmospheric; feed H_2 to C_2H_4 molar ratio 4:1 or feed H_2 to D_2 molar ratio 1:1). Thus, we infer that the inhibition by CO was so strong that these catalysts were completely poisoned. However, when only one CO ligand was present with ethylene on the rhodium—formed from the rhodium dicarbonyl as the catalyst was exposed to a stream of $C_2H_4 + H_2$ or $C_2H_4 + H_2 + D_2$—the activities for ethylene conversion and for H−D exchange were greater (Table 2). When, instead of two CO ligands, the rhodium was bonded to two ethylene ligands and no CO, the activity was still greater (Table 2). Thus, the more CO, the greater the inhibition.

The zeolite-supported rhodium carbonyl complexes, after incorporation of C_2H_4 ligands replacing CO ligands, were investigated in detail as catalysts for the conversion of ethylene in the presence of H_2. Conversion data were determined with the once-through isothermal plug-flow reactor for the catalyst with one CO ligand instead of ethylene and for the catalyst with two ethylene ligands instead of CO.

Plots of conversion as a function of time on stream (Figures 1A and 2A) include for comparison data of Serna et al.[22−27] characterizing the catalyst initially in the form of $Rh(C_2H_4)_2$/HY zeolite (Figures 1A and S10−S12). The data were extrapolated to zero time on stream to determine initial conversions; the extrapolations were done on semilogarithmic plots (Figure 1A), with the data being well represented by straight lines.

In contrast, the time-on-stream performance of the catalyst initially in the form of $Rh(CO)(C_2H_4)$ complexes underwent an initial activation followed by near-steady-state performance; the extrapolation to determine the initial activity is illustrated in Figure 2A.

The intent of the extrapolations was to determine catalyst performance for the initial ligand environments of the metals (which we determined spectroscopically). The values of the initial conversions were plotted as a function of inverse space velocity, as illustrated in Figure S11. These plots are linear and, within error, pass through the origin, demonstrating that the conversions were differential, determining reaction rates

DOI: 10.1021/acscatal.5b00995
ACS Catal. 2015, 5, 5647−5656

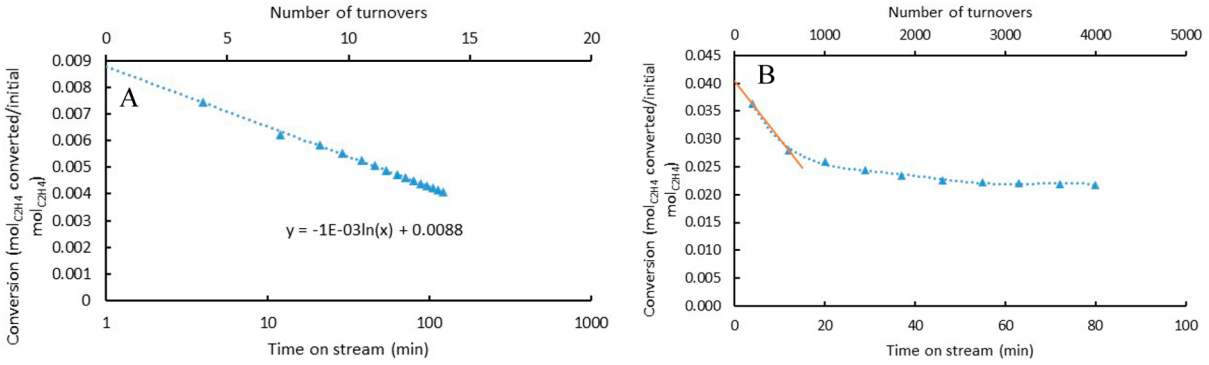

Figure 4. Performance of initially incorporating $Ir(CO)(C_2H_4)$ complexes supported on HY zeolite in a plug-flow reactor, with illustrations of the extrapolations to determine initial conversions. The data were obtained at atmospheric pressure and at (A) 300 K and (B) 373 K. The gas feed flow rates were 40 mL/min of H_2, 10 mL/min of ethylene, and with balance helium of 50 mL/min of helium; the catalyst mass was 240 mg for measurements at 300 K and 4 mg for measurements at 373 K. The iridium content 1 wt %.

directly as the slopes of the lines. These rates were used to determine turnover frequencies (TOF), as in earlier work.[22−27] The errors in these values (Table 2) were estimated on the basis of data from repeat experiments and estimates of the uncertainties in the conversions, catalyst metal contents, and reactant flow rates.

The initial TOF data are compared with reported results in Table 2 and Figures S12 and S13. Table 2 includes selectivities in the conversion of ethylene to dimers as well as ethane.

The data characterizing the $H_2 + D_2$ reaction were determined in the IR cell/flow reactor, with the effluent stream analyzed by mass spectrometry. The conversions were calculated after 8 min of contact with $C_2H_4 + H_2 + D_2$ in 1:2:2 molar ratios, after the HD signal had become essentially constant. After 8 min, the gas stream was sent to a bypass for 1 min to determine the difference between the mass spectrometer signal of the product and that of the ethylene + H_2 + D_2 feed mixture (Table 2).

In contrast to the pattern observed for the ethylene conversion, the H−D exchange activity was greater for the $Rh(CO)(C_2H_4)$ complex than for the $Rh(C_2H_4)_2$ complex; the conversion increased from 3.5 to 7.3% as a result of incorporation of the CO ligand replacing an ethylene ligand.

CO also influenced the selectivity of the catalysts for ethylene conversion. The selectivity for dimerization at zero time on stream and 300 K decreased from 65 to 10% (Figure 2) when one ethylene ligand was replaced by CO.

Performance of Supported Iridium Complex Catalysts. Results characterizing the catalytic performance of the zeolite-supported iridium complexes under the same conditions as those applied for the rhodium catalysts (Table 2 and Figures 3, 4) show that the catalyst incorporating $Ir(CO)_2$, like that incorporating $Rh(CO)_2$, was inactive under our conditions.

Data illustrating the time-on-stream performance representing the other supported iridium complex catalysts are shown in Figures 3 and 4 and S14−S18. The extrapolations to determine the initial turnover frequencies are shown in Figures 3, 4, S15, S17, and S18. The patterns of activity and selectivity with time-on-stream are not the same as those observed for the rhodium catalysts.

The extrapolated data determine the initial TOF values summarized in Table 2. These data show that, comparable to the rhodium-containing catalysts, the catalyst that initially incorporated $Ir(CO)(C_2H_4)_2$ was less active than the one that initially incorporated $Ir(C_2H_4)_2$, again demonstrating the role of CO as an inhibitor. In the ethylene conversion, the catalyst initially present as $Ir(CO)(C_2H_4)$ was 2 orders of magnitude lower in activity than that initially present as $Ir(C_2H_4)_2$ at room temperature, and correspondingly the activity for H−D exchange was also less.

Besides decreasing the activity, the CO ligands also markedly affected the selectivity of the supported iridium catalysts (Table 2), with the catalyst initially present as $Ir(C_2H_4)_2$ complexes having a dimerization selectivity of 11% compared with 0% when the CO ligand was present.

Comparison of Initial Performances of Rhodium Complex and Iridium Complex Catalysts. The data show that the rhodium complex catalyst initially incorporating one CO and one ethylene ligand was an order of magnitude more active than the isostructural iridium complex for ethylene hydrogenation at 300 K. At 373 K, the $Rh(CO)(C_2H_4)$ complexes were so active that it was not possible with our apparatus to obtain conversions in the differential range to compare with those of the less active $Ir(CO)(C_2H_4)$ species; however, as was observed at 300 K, the $Rh(CO)(C_2H_4)$ species at 373 K were more active for ethylene hydrogenation than the $Ir(CO)(C_2H_4)$ species. The $Rh(CO)(C_2H_4)$ species were active for dimerization at 300 K, but the isostructural iridium species were not.

The comparisons for H−D exchange are available in terms of conversions but not initial TOF values, because the conversions were often greater than differential. At 300 K, the conversion observed for the $Rh(CO)(C_2H_4)$ species was 7.3% and that for the isostructural iridium complex was 3.4%, in qualitative accord with the relative activities for ethylene hydrogenation. Likewise, at 373 K the conversion for the H−D exchange observed with this rhodium carbonyl complex was greater than that for the isostructural iridium carbonyl complex (66% vs 36%), again in qualitative agreement with the pattern for ethylene hydrogenation, consistent with the expectation that H_2 activation is needed for ethylene hydrogenation.[7,27,28]

Although the H−D exchange activities of the catalysts initially present as $Rh(C_2H_4)_2$ and $Ir(CO)(C_2H_4)$ are approximately the same (Table 2), their activities for ethylene hydrogenation are markedly different, a result that demonstrates the subtlety of influence of the CO ligand.

Changes in Catalysts during Operation. Each of the catalysts, except the one incorporating $Rh(CO)(C_2H_4)$ species, underwent deactivation during operation (Figures 1−4). During deactivation, it was observed that deposits accumulated

DOI: 10.1021/acscatal.5b00995
ACS Catal. 2015, 5, 5647−5656

on the surfaces of the catalysts, making them a little darker; these are inferred to be hydrocarbons (evidenced by intense IR bands in the range 2964−2876 cm^{-1}, Figure S19), in agreement with previous work characterizing catalysts initially present as $M(C_2H_4)_2$ species.[7,22,27] In contrast, such a change was not observed for the catalyst initially present as $Rh(CO)(C_2H_4)$ species that did not undergo substantial deactivation during 350 min of contact with H_2 and C_2H_4.

The absence of EXAFS evidence of metal−metal bonds in the supported species after longer exposure to the reactants has been demonstrated (within the sensitivity of the technique) for this class of materials and similar experimental conditions.[22−27] Metal carbonyl species are known to bond strongly to the acidic Al sites of the zeolite, resisting aggregation even in pure H_2 streams at elevated temperatures.[32]

The selectivity for ethylene dimer formation distinguishes the catalysts as follows: at 300 K, the selectivity of the catalyst initially present as $Ir(C_2H_4)_2$ complexes increased from the beginning of operation until it nearly reached a steady state after 150 min (Figure 3B). In contrast, the catalyst initially in the form of $Ir(CO)(C_2H_4)$ complexes was inactive for ethylene dimerization at 300 and at 373 K, and this lack of activity was maintained as long as the catalyst was in operation.

In further contrast, the selectivity for ethylene dimer formation of the catalyst initially present as $Rh(C_2H_4)_2$ complexes underwent a slow decrease in operation at room temperature (Figure 1B), but the selectivity of the catalyst initially present as $Rh(CO)(C_2H_4)$ complexes was almost constant during the apparent "activation" period and then increased (Figure 2) after the activity attained a near steady state.

The changing selectivities and activities of the catalysts in operation suggest that there were changes in the ligands bonded to the metals during operation, and IR spectra were measured to track those changes, as described next.

Identification of Supported Rhodium Complexes Present during Catalysis. The CO ligands in the metal complexes are sensitive indicators of the other ligands bonded to the metals. Thus, IR spectra of the functioning catalysts incorporating CO ligands provide evidence of the changing ligands as the catalyst initially present as $Rh(CO)(C_2H_4)$ complexes evolved from the initial form. Spectra characterizing the catalyst (33 mg with 1 wt % rhodium) under reaction conditions (40 mL/min of H_2, 10 mL/min of ethylene, and 50 mL/min of helium) at 298 K and atmospheric pressure, Figure 5, include a band at 2056 cm^{-1}, assigned to the initial $Rh(CO)(C_2H_4)$ complexes,[6] and one at 2063 cm^{-1}, also observed when only ethylene flowed through the reactor (Figure S7), assigned to rhodium carbonyl species interacting with ethylene. The intensities of these two bands changed during catalysis, as follows: after 22 min, the 2056 cm^{-1} band still predominated, but there was a shoulder at 2063 cm^{-1}. During the first 95 min of contact with $H_2 + C_2H_4$, the intensity of the latter band had increased further, accompanied by an increase in the catalytic activity for ethylene conversion (Figure 2A) and a nearly constant selectivity for dimers (Figure 2B).

After 180 min, the overall activity had reached a near steady state (Figure 2A), but the selectivity started to increase (Figure 2B), and the 2063 cm^{-1} band (assigned to rhodium carbonyl species interacting with ethylene) was blue-shifted by 2 cm^{-1} and increased in intensity as the band at 2056 cm^{-1} (assigned to $Rh(CO)(C_2H_4)$ species) concomitantly decreased further in intensity. These results suggest that the band at 2063 cm^{-1} assigned to rhodium carbonyl species interacting with ethylene could be a reaction intermediate in the ethylene dimerization reaction.

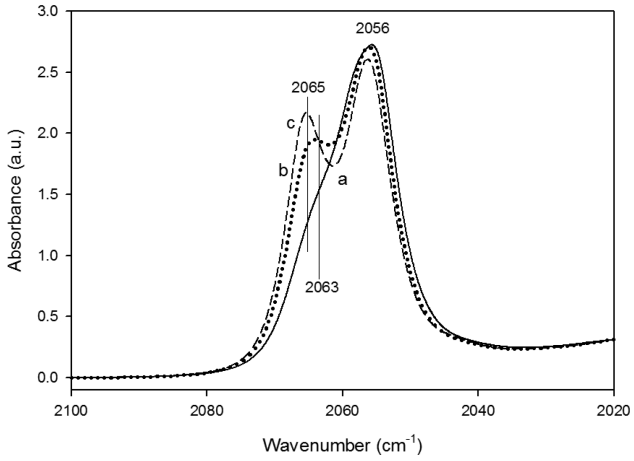

Figure 5. IR spectra of a sample initially in the form of $Rh(CO)(C_2H_4)$/HY zeolite in flowing $H_2 + C_2H_4$ with a H_2/C_2H_4 ratio of 4:1 at 298 K and 1 bar after the following times (min): (a, solid line) 22, (b, dotted line) 95, and (c, dashed line) 180.

Experiments were also carried out with feeds including $H_2 + D_2 + C_2H_4$. Mass spectra of the products show the presence of deuterated ethane (C_2H_5D and $C_2H_4D_2$) and the fragments corresponding to butenes (C_3H_5 and C_4H_8) with no deuterated dimers. These observations are consistent with expectation[16] and the inference[16] that the dimer formation proceeds via ethylene ligands on the rhodium and the hydrogenation via ethyl ligands. Thus, we infer that the CO ligand on the rhodium does not affect the reaction pathway.

When the $Rh(CO)(C_2H_4)$ complexes were brought in contact with $H_2 + C_2H_4$ at 373 K, the IR spectra (Figure S20) show the disappearance of the $Rh(CO)(C_2H_4)$ band (at 2056 cm^{-1}) with the concomitant appearance of bands assigned to $Rh(CO)_2$ species (at 2117 and 2053 cm^{-1}) and, we postulate on the basis of previous work,[6] Rh(CO)(H) species (at 2093 cm^{-1}). The appearance of rhodium hydride species accompanied by a high activity for H_2 activation is in agreement with the high hydrogenation activity, which is accompanied by a reduction of the activity for the dimerization pathway. Our experience with these and related samples indicates that metal clusters do not form under our reaction conditions, and so the IR bands observed after the various treatments are assigned to mononuclear metal complexes coordinated to various sets of ligands.[6,33] Under our conditions, the ethylene evidently did not interact substantially with the acidic sites of the zeolite when the catalyst incorporated what we infer to be Rh(CO)(H) species (as shown by the IR data, Figure S20A), in contrast with what was observed with the $Rh(C_2H_4)_2$[27] and $Rh(CO)(C_2H_4)$ species (Figure S21), which are both active for ethylene dimerization.

Identification of Supported Iridium Complexes Present during Catalysis. IR spectra recorded during catalysis also provide information about the supported iridium complexes. The spectra of the carbonyl-containing iridium complexes, initially $Ir(CO)(C_2H_4)$, at 298 K (Figure 6) show bands at 2087 and 2054 cm^{-1}, assigned to $Ir(CO)(C_2H_4)_2$ and $Ir(CO)(C_2H_4)$, respectively. At 298 K and at 373 K, the iridium carbonyl complexes catalyzed ethylene hydrogenation without measurable oligomerization (Table 2). The spectra recorded

DOI: 10.1021/acscatal.5b00995
ACS Catal. 2015, 5, 5647−5656

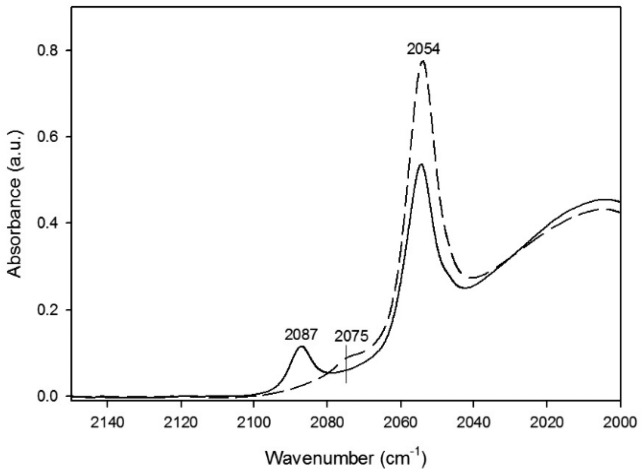

Figure 6. IR spectra of $Ir(CO)(C_2H_4)$/HY zeolite in flowing H_2 + C_2H_4 at a 4:1 ratio at 298 K (solid line) and at 373 K (dashed line) and 1 atm. Spectra taken after 6 min of contact with H_2 + C_2H_4. The intensities of the bands did not change substantially during the first 60 min of reaction.

during catalysis at 373 K (Figure 6) include both the band assigned to $Ir(CO)(C_2H_4)$ and a band at 2075 cm^{-1} assigned[33] to $Ir(CO)(C_2H_5)$ complexes.

Thus, at 373 K, the evidence of the hydrogenated species $Ir(CO)(C_2H_5)$ points to a reaction intermediate for ethylene hydrogenation, although there is no spectroscopic evidence of it at 298 K; instead, there is evidence of $Ir(CO)(C_2H_4)_2$ complexes (although there is no such evidence recorded during catalysis at 373 K). Correspondingly, there was a marked difference between the catalytic activity for ethylene hydrogenation of the catalysts at 298 and 373 K, with TOF values of 0.005 and 1.52 s^{-1}, respectively. Therefore, we infer that the $Ir(CO)(C_2H_4)_2$ species that was present at 298 K was barely if at all involved in the ethylene hydrogenation reaction and that ethylene acted as a reaction inhibitor. This inference is in agreement with reports[4] showing that iridium complexes bonded to the zeolite surface and simultaneously to three ligands (18-e$^-$ species) are unreactive for the dissociation of H_2, and thus lack catalytic hydrogenation activity.

Hydrogenation of ethylene by $Ir(C_2H_4)_2$ species also proceeded with ethyl as an intermediate, observed by IR spectroscopy, and as reported previously.[8] Thus, in this case also, we infer that the CO ligand did not block the reaction pathway.

During reaction in an atmosphere of H_2 + ethylene with feed flow rates of 40 mL/min of H_2, 10 mL/min of ethylene, and 50 mL/min of helium, the $Ir(CO)(C_2H_4)$ at 373 K was observed to be highly active for H_2 activation (as shown by the H−D exchange activity, Table 2), and in this case, the activated hydrogen evidently hindered the interaction of ethylene from the gas phase with the zeolite, as evidenced by the lack of a decrease in intensity of the Al−OH bands at 3630 and 3566 cm^{-1} (Figure S22), which otherwise resulted from bonding of ethylene with these groups (Figure S21).

DISCUSSION

The data presented here are unique in determining the roles of systematically varied ligands in isostructural supported rhodium and supported iridium catalysts. They show clearly that the strongly bonded CO ligand is a strong inhibitor: when the initial species present in the catalyst was either $Rh(CO)_2$ or $Ir(CO)_2$, the catalysts were inactive. Thus, we infer that the initial species, which were four-coordinate metal complexes (with two ligands being CO and two being oxygen atoms of the support) under our catalytic reaction conditions did not react substantially to coordinate both ethylene and hydrogen or both hydrogen and deuterium, along with the two CO ligands, to give species with measurable catalytic activity.

In contrast, after the $M(CO)_2$ species were brought in contact with ethylene and H_2, so that one of the CO ligands was replaced by ethylene to give $M(CO)(C_2H_4)$ species, catalysis was observed. The supported metal complexes incorporating one CO and one ethylene ligand were catalytically active for both ethylene hydrogenation and the reaction of H_2+ D_2 to give HD (Table 2).

When no CO ligand was present, each metal complex was then more active (Table 2). Thus, the overall activity at room temperature followed the trend $M(C_2H_4)_2$ > $M(CO)(C_2H_4)$ > $M(CO)_2$, demonstrating the inhibition by the CO ligand.

The seemingly unusual catalytic behavior of the $Rh(CO)(C_2H_4)$ species (among the others considered in this work) at 300 K (Figure 2) and the correlated IR spectra (Figure 5) led to the data summarized in Figure 7. The dimerization activity

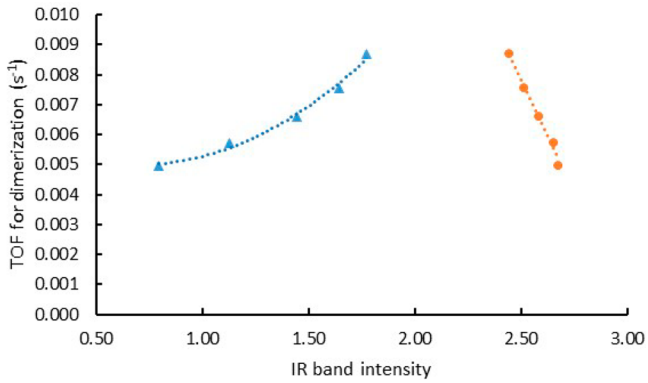

Figure 7. Dependence of turnover frequency for dimerization on the intensities of two IR bands (a.u.) for reaction catalyzed by a sample initially in the form of $Rh(CO)(C_2H_4)$/HY zeolite. Reaction conditions: flowing H_2 + C_2H_4 in 4:1 molar ratio at 298 K and 1 bar. The data represent the $Rh(CO)(C_2H_4)$ band at 2056 cm^{-1} (●) and the band at 2063 cm^{-1} assigned to intermediates in the dimerization (▲).

increased as the intensity of the band at 2063 cm^{-1} increased, a result that suggests that this band represents rhodium carbonyl complexes that are intermediates in the dimerization reaction.

An advantage of having one CO ligand on the catalytic metal complex is that it facilitated identification by IR spectroscopy of the predominant species present during catalysis and, because of the sensitivity of the C−O stretching frequency to the other ligands on the metal, elucidation of evidence of the electron density on the metal centers.

At room temperature, the supported rhodium complexes that incorporated only one ethylene ligand when CO was also present as a ligand were found to be active for ethylene dimerization. Previous work with 4-coordinated rhodium diethylene complexes also shows the striking effects that various ligands, other than ethylene, have on the electronic environment around the rhodium and thus its behavior in reactive atmospheres.[34] In contrast, the iridium carbonyl complexes accommodate not only one but two ethylene

DOI: 10.1021/acscatal.5b00995
ACS Catal. 2015, 5, 5647−5656

ligands—and they were found not to be active for ethylene dimerization. These results are consistent with an earlier inference[27] that ethylene dimerization occurs via the interaction of the ethylene ligands bonded to rhodium with ethylene ligands (or species formed from them) bonded to the acidic sites of the zeolite support[27]—rather than via two ethylene ligands bonded to a rhodium center. Because the supports were the same for the two metals, thus able to bond to ethylene nearby metal centers incorporating ethylene ligands, we suggest that the lack of activity of the iridium complexes for ethylene dimer formation is a consequence of the different bonding of ethylene to iridium vs rhodium (an inference that is bolstered by the observed tendency of the former but not the latter to bond to two ethylene ligands). Moreover, $Ir(C_2H_4)_2$ complexes have a high activity for H−D exchange, which suggests that the H_2 spilled over from iridium onto the support hinders the interaction between ethylene and the support that inhibits the dimerization activity, as was observed previously for rhodium when the H_2 activation was sufficiently boosted (for example, as small rhodium clusters formed on the zeolite surface).[22]

The ν_{CO} frequencies probe the electron density on the metals: the higher the frequency of the ν_{CO} vibration, the weaker the M−CO bond and correspondingly the stronger the backbonding of other π-acid ligands such as ethylene.[35] The C−O bands characterizing the $M(CO)(C_2H_4)$ complexes are nearly the same for rhodium and iridium, 2056 and 2054 cm^{-1}, respectively. This comparison suggests that the electronic effect of the CO on the π-bonded ethylene ligands was nearly the same for the rhodium and iridium in our catalysts.

The spectra demonstrate a significant difference in electron density between rhodium and iridium complexes when they incorporate reaction intermediates. The ν_{CO} frequencies were found to be 2063 cm^{-1} for the rhodium carbonyl complex, which we infer to be a reaction intermediate, and 2075 cm^{-1} for the iridium carbonyl complex $Ir(CO)(C_2H_5)$. The difference in the M−CO frequencies characterizing these rhodium and iridium complexes is an indication of different electron densities around the metals under reaction conditions, which is related to the differences in bonding of ligands other than CO.[36,37] Hence, we infer that the differences between rhodium and iridium in bonding hydrogen and ethylene affect the catalytic activities (Table 2), but we recognize that this is not a sufficient explanation for the differences in catalytic properties of the rhodium and iridium complexes.

Reduction and aggregation of the metals under our catalytic reaction conditions (in contact with H_2 and ethylene) were negligible. Supported iridium complexes incorporating two ethylene ligands do not undergo significant aggregation at room temperature, but they start to aggregate at 80 °C when in contact with pure H_2, as has been characterized by IR and EXAFS spectroscopies.[29] On the other hand, supported rhodium diethylene complexes form clusters after 1 h of contact with pure H_2 at room temperature.[22] Reversible cluster formation and breakup involving zeolite-supported organometallics, initially present as mononuclear complexes, has been characterized in real time by IR and EXAFS spectroscopies, with metal−metal coordination numbers indicated by the EXAFS spectra and evidence of the changing ligands on the metal evidenced by both IR and EXAFS spectra, and evidence of changes in the metal−support interface evidenced by both kinds of spectra.[38] Thus, it is evident that H_2 is a reducing agent that facilitates cluster formation from mononuclear iridium complexes, and ethylene is an oxidizing agent that facilitates cluster breakup. A balance between complexes and clusters can be regulated by the ratio of H_2 to ethylene in the gas phase.[38] The IR and EXAFS data characterizing our samples give evidence of mononuclear iridium complexes under our catalytic reaction conditions, with no evidence of iridium cluster formation. IR spectra of one of our catalysts, for example, after exposure to a pulse of CO after catalysis in the flow reactor (Figure S23) lack evidence of CO bridging bands that would be indicative of neighboring iridium centers (clusters), instead indicating terminal ligands and mononuclear iridium.

Metal carbonyl species are known to resist aggregation even when in contact with pure H_2 at elevated temperatures.[32] Because the aim of this work was to compare mononuclear complexes and not clusters, no treatments with pure H_2 were performed.

The ability of the species to undergo decarbonylation is correlated with some catalytic observations. For example, iridium dicarbonyl species do not decarbonylate easily on electron-donating supports such as MgO, and then these species are inactive in H/D exchange reactions,[29] whereas the same species on the electron-withdrawing zeolite undergo replacement of one CO ligand by ethylene—and show some activity for the HD exchange. This behavior is correlated with the effect of the support as a ligand affecting the electron-density on the metal and, thus, its capacity to accommodate various ligands for catalytic reactions.

Taken together, our data provide one of the clearest comparisons of two metals in the form of supported mononuclear catalysts.

CONCLUSIONS

In summary, well-defined zeolite-supported rhodium and iridium complexes incorporating a family of species including $M(CO)_2$, $M(CO)(C_2H_4)$, and $M(C_2H_4)_2$ complexes were tested as catalysts for the conversion of ethylene and H_2. IR and X-ray absorption spectra provide structural characterizations of the catalyst precursors, with IR spectra providing evidence of the species present as ligands during catalysis. The role of the CO is not only to occupy bonding sites on the metal and thus inhibit the catalytic reactions but also to influence the bonding of the other ligands to the metal and therefore affect the catalyst performance. The data presented here are unique in providing comparisons of the catalytic activities of isostructural rhodium and iridium complexes and determining intrinsic differences between the two metals, illustrated in part by the frequencies of the CO stretching vibrations in the isostructural complexes. We stress that the measurements and conclusions reported here were possible only because of the near-uniformity of the supported species, which are molecular analogues, which allow a precise characterization of the species involved during catalysis.

ASSOCIATED CONTENT

Supporting Information

The Supporting Information is available free of charge on the ACS Publications website at DOI: 10.1021/acscatal.5b00995.

Experimental details and additional spectra (PDF)

AUTHOR INFORMATION

Corresponding Author

*E-mail: bcgates@ucdavis.edu.

DOI: 10.1021/acscatal.5b00995
ACS Catal. 2015, 5, 5647−5656

Notes

The authors declare no competing financial interest.

■ ACKNOWLEDGMENTS

We thank Adam Hoffman for help with the EXAFS data presentation. This work was supported by the U.S. Department of Energy (DOE), Office of Science, Basic Energy Sciences (BES), Grant DE-FG02-04ER15513 (C.M.M.). C.M.M. was supported in part by the UC-MEXUS-CONACYT doctoral fellowship program. This research was aided by resources of the Advanced Photon Source, a DOE Office of Science User Facility operated for the DOE Office of Science by Argonne National Laboratory (ANL) under Contract No. DE-AC02-06CH11357. Experiments were performed at beamline 10-ID-B (the MRCAT) at ANL; MRCAT operations are supported by the DOE and the MRCAT member institutions. We thank HPCAT (Sector 16) of APS for access to a glovebox for sample preparation and storage during our beam time. HPCAT operations are supported by DOE-NNSA under Award No. DE-NA0001974 and DOE-BES under Award No. DE-FG02-99ER45775, with partial instrumentation funding by NSF. APS is supported by DOE-BES under Contract No. DE-AC02-06CH11357. We acknowledge beam time at beamline 4-1 at the Stanford Synchrotron Radiation Lightsource supported by the DOE Division of Materials Sciences. We thank the beamline staffs for valuable support.

■ REFERENCES

(1) Miessner, H. *J. Am. Chem. Soc.* **1994**, *116*, 11522−11530.
(2) Qiao, B.; Wang, A.; Yang, X.; Allard, L. F.; Jiang, Z.; Cui, Y.; Liu, J.; Li, J.; Zhang, T. *Nat. Chem.* **2011**, *3*, 634−641.
(3) Serna, P.; Gates, B. C. *Acc. Chem. Res.* **2014**, *47*, 2612−2620.
(4) Campbell, C. T.; Peden, C. H. F. *Science* **2005**, *309*, 713−714.
(5) Fu, Q.; Saltsburg, H.; Flytzani-Stephanopoulos, M. *Science* **2003**, *301*, 935−938.
(6) Liang, A. J.; Craciun, R.; Chen, M.; Kelly, T. G.; Kletnieks, P. W.; Haw, J. F.; Dixon, D. A.; Gates, B. C. *J. Am. Chem. Soc.* **2009**, *131*, 8460−8473.
(7) Lu, J.; Serna, P.; Gates, B. C. *ACS Catal.* **2011**, *1*, 1549−1561.
(8) Dixon, D. A.; Chen, M. Private communication, 2014.
(9) Davis, R. J.; Rossin, J. A.; Davis, M. E. *J. Catal.* **1986**, *98*, 477−486.
(10) Astruc, D. In *Organometallic Chemistry and Catalysis*; Springer-Verlag: Berlin, 2007; p 151.
(11) Kroner, A. B.; Newton, M. A.; Tromp, M.; Roscioni, O. M.; Russell, A. E.; Dent, A. J.; Prestipino, C.; Evans, J. *ChemPhysChem* **2014**, *15*, 3049−3059.
(12) Panayotov, D.; Mihaylov, M.; Nihtianova, D.; Spassov, T.; Hadjiivanov, K. *Phys. Chem. Chem. Phys.* **2014**, *16*, 13136−13144.
(13) Anselment, T. M. J.; Vagin, S. I.; Rieger, B. *Dalton Trans.* **2008**, *34*, 4537−4548.
(14) Yardimci, D.; Serna, P.; Gates, B. C. *ChemCatChem* **2012**, *4*, 1547−1550.
(15) Weitkamp, J. *ChemCatChem* **2012**, *4*, 292−306.
(16) Lefebvre, F. In *Atomically-Precise Methods for Synthesis of Solid Catalysts*, RSC Catalysis Series; Hermans, S., de Bocarmé, T. V., Eds.; RSC: Cambridge, UK, 2015; p 1.
(17) Bhirud, V. A.; Uzun, A.; Kletnieks, P. W.; Craciun, R.; Haw, J. F.; Dixon, D. A.; Olmstead, M. M.; Gates, B. C. *J. Organomet. Chem.* **2007**, *692*, 2107−2113.
(18) Odzak, J. F.; Argo, A. M.; Lai, F. S.; Gates, B. C. *Rev. Sci. Instrum.* **2001**, *72*, 3943−3945.
(19) Miessner, H.; Gutschick, D.; Ewald, H.; Muller, H. *J. Mol. Catal.* **1986**, *36*, 359−373.
(20) Yates, J. T., Jr.; Duncan, T. M.; Worley, S. D.; Vaughan, R. W. *J. Chem. Phys.* **1979**, *70*, 1219−1225.
(21) Teo, B. K. *J. Am. Chem. Soc.* **1981**, *103*, 3990−4001.
(22) Serna, P.; Gates, B. C. *J. Am. Chem. Soc.* **2011**, *133*, 4714−4717.
(23) van Veen, J. A.; Jonkers, G.; Hesselink, W. H. *J. Chem. Soc., Faraday Trans. 1* **1989**, *85*, 389−413.
(24) van Der Voort, P.; White, M. G.; Vansant, E. F. *Langmuir* **1998**, *14*, 106−112.
(25) Uzun, A.; Bhirud, V. A.; Kletnieks, P. W.; Haw, J. F.; Gates, B. C. *J. Phys. Chem. C* **2007**, *111*, 15064−15073.
(26) Liang, A. J.; Bhirud, V. A.; Ehresmann, J. O.; Kletnieks, P. W.; Haw, J. F.; Gates, B. C. *J. Phys. Chem. B* **2005**, *109*, 24236−24243.
(27) Serna, P.; Gates, B. C. *Angew. Chem., Int. Ed.* **2011**, *50*, 5528−5531.
(28) Lu, J.; Martinez-Macias, C.; Aydin, C.; Browning, N. D.; Gates, B. C. *Catal. Sci. Technol.* **2013**, *3*, 2199−2203.
(29) Lu, J.; Serna, P.; Aydin, C.; Browning, N. D.; Gates, B. C. *J. Am. Chem. Soc.* **2011**, *133*, 16186−16195.
(30) Hayden, B. E.; King, A.; Newton, M. A. *Surf. Sci.* **1998**, *397*, 306−313.
(31) Newton, M. A.; Evans, J.; Hayden, B. E. *J. Phys. Chem. B* **2000**, *104*, 8548−8553.
(32) Serna, P.; Yardimci, D.; Kistler, J. D.; Gates, B. C. *Phys. Chem. Chem. Phys.* **2014**, *16*, 1262−1270.
(33) Martinez-Macias, C.; Chen, M.; Dixon, D. A.; Gates, B. C. *Chem. - Eur. J.* **2015**, *21*, 11825−11835.
(34) Cramer, R. *J. Am. Chem. Soc.* **1964**, *86*, 217−222.
(35) van Leeuwen, P. W. N. M.; van Koten, G. In *Catalysis: An Integrated Approach to Homogeneous, Heterogeneous, and Industrial Catalysis*; Moulijn, J. A., van Leeuwen, P. W. N. M., van Santen, R. A., Eds.; Elsevier: Amsterdam, 1993; p 221.
(36) Fohlisch, A.; Nyberg, M.; Bennich, P.; Triguero, L.; Hasselstrom, J.; Karis, O.; Pettersson, L. G. M.; Nilsson, A. *J. Chem. Phys.* **2000**, *112*, 1946−1958.
(37) Hadjiivanov, K. I.; Vayssilov, G. N. *Adv. Catal.* **2002**, *47*, 307−511.
(38) Uzun, A.; Gates, B. C. *Angew. Chem., Int. Ed.* **2008**, *47*, 9245−9248.

DOI: 10.1021/acscatal.5b00995
ACS Catal. 2015, 5, 5647−5656